Optimization of a Glucagon-Like Peptide 1 Receptor Antagonist Antibody for Treatment of Hyperinsulinism

Sean M. Peterson,[1] Christine A. Juliana,[2] Cameron F. Hu,[1] Jinghua Chai,[2] Carson Holliday,[1] Kara Y. Chan,[1] Ana G. Lujan Hernandez,[1] Zoe Challocombe,[1] Linya Wang,[1] Zhen Han,[1] Nikhil Haas,[1] Ryan Stafford,[1] Fumiko Axelrod,[1] Tom Z. Yuan,[1] Diva D. De León,[2,3] and Aaron K. Sato[1]

Diabetes 2023;72:1320–1329 | https://doi.org/10.2337/db22-1039

Congenital hyperinsulinism (HI) is a genetic disorder in which pancreatic β-cell insulin secretion is excessive and results in hypoglycemia that, without treatment, can cause brain damage or death. Most patients with loss-of-function mutations in *ABCC8* and *KCNJ11*, the genes encoding the β-cell ATP-sensitive potassium channel (K_{ATP}), are unresponsive to diazoxide, the only U.S. Food and Drug Administration–approved medical therapy and require pancreatectomy. The glucagon-like peptide 1 receptor (GLP-1R) antagonist exendin-(9-39) is an effective therapeutic agent that inhibits insulin secretion in both HI and acquired hyperinsulinism. Previously, we identified a highly potent antagonist antibody, TB-001-003, which was derived from our synthetic antibody libraries that were designed to target G protein–coupled receptors. Here, we designed a combinatorial variant antibody library to optimize the activity of TB-001-003 against GLP-1R and performed phage display on cells overexpressing GLP-1R. One antagonist, TB-222-023, is more potent than exendin-(9-39), also known as avexitide. TB-222-023 effectively decreased insulin secretion in primary isolated pancreatic islets from a mouse model of hyperinsulinism, *Sur1*$^{-/-}$ mice, and in islets from an infant with HI, and increased plasma glucose levels and decreased the insulin to glucose ratio in *Sur1*$^{-/-}$ mice. These findings demonstrate that targeting GLP-1R with an antibody antagonist is an effective and innovative strategy for treatment of hyperinsulinism.

ARTICLE HIGHLIGHTS

- Patients with the most common and severe form of diazoxide-unresponsive congenital hyperinsulinism (HI) require a pancreatectomy. Other second-line therapies are limited in their use because of severe side effects and short half-lives.
- Therefore, there is a critical need for better therapies. Studies with the glucagon-like peptide 1 receptor (GLP-1R) antagonist, avexitide (exendin-(9-39)), have demonstrated that GLP-1R antagonism is effective at lowering insulin secretion and increasing plasma glucose levels.
- We have optimized a GLP-1R antagonist antibody with more potent blocking of GLP-1R than avexitide.
- This antibody therapy is a potential novel and effective treatment for HI.

Congenital hyperinsulinism (HI) is a genetic disorder of the pancreatic β-cells that causes excessive insulin secretion and persistent hypoglycemia. The most common and severe form of HI is caused by inactivating mutations in *ABCC8* or *KCNJ11*, the genes encoding the two subunits of β-cell ATP-sensitive potassium channels (K_{ATP}) SUR1 and Kir6.2, respectively (1,2). Loss-of-function mutations in the K_{ATP} channel results in unregulated plasma membrane depolarization, elevated intracellular calcium levels, and dysregulated insulin secretion (3,4). The only U.S. Food and Drug Administration–approved treatment for HI, diazoxide, suppresses insulin secretion by promoting the opening of K_{ATP} channels and repolarizing of the plasma membrane; thus, it

[1]Twist Bioscience, South San Francisco, CA
[2]Division of Endocrinology and Diabetes, The Children's Hospital of Philadelphia, Philadelphia, PA
[3]Department of Pediatrics, Perelman School of Medicine at the University of Pennsylvania, Philadelphia, PA

Corresponding authors: Diva D. De Leon, deleon@chop.edu, and Aaron K. Sato, asato@twistbioscience.com

Received 20 December 2022 and accepted 13 June 2023

This article contains supplementary material online at https://doi.org/10.2337/figshare.23550024.

S.M.P. and C.A.J. contributed equally to this work.

is ineffective in most patients with K_{ATP}-HI. For diazoxide-unresponsive cases with diffuse histology, a near-total pancreatectomy may be required to treat persistent hypoglycemia (2,5,6). However, pancreatectomy may only partially control the hypoglycemia and can result in development of diabetes later in life (6). Thus, there is a critical need for development of safe and effective therapies for treatment of HI.

The K_{ATP}-HI mouse model, *Sur1*$^{-/-}$ mice, targets inactivation of the *Sur1* gene and demonstrates key pathophysiological features of human K_{ATP}-HI. Because of loss-of-function of the K_{ATP} channels, β-cells in *Sur1*$^{-/-}$ mice cannot suppress insulin output during a fall in glucose concentration, leading to fasting hypoglycemia, and the cells exhibit loss of first-phase insulin secretion resulting in glucose intolerance (7,8). By perifusion, primary isolated pancreatic *Sur1*$^{-/-}$ islets exhibit all the characteristics expected of nonfunctional K_{ATP} channels, including membrane depolarization and elevated intracellular calcium levels (8–10). *Sur1*$^{-/-}$ islets also secrete insulin in response to amino acid stimulation consistent with the protein-induced hypoglycemia found in patients with K_{ATP}-HI (9,11,12).

The glucagon-like peptide 1 receptor (GLP-1R) antagonist exendin-(9-39) inhibits insulin secretion (13,14) in human and mouse islets lacking functional K_{ATP} channels. GLP-1R is activated by metabolites of the GLP-1 peptide, as well as exendins, which are exogenous peptides extracted from *Heloderma horridum* venom (15). GLP-1 and exendin peptides form α-helical rods that bind to the orthosteric binding pocket observed in most G protein–coupled receptors (GPCRs) (16). GLP-1 and exendin peptides also bind to a unique N-terminal domain found in the class B (secretin) GPCR family (17). However, exendin and GLP-1 peptides are also metabolized into truncated forms, which bind to the N-terminal domain, but not the orthosteric binding pocket, and function as antagonists (18). Exendin-4 is the full-length exendin peptide that displays full agonism at GLP-1R. Exendin-(9-39), a truncated derivative of the exendin-4 peptide, binds the N-terminal domain and acts as a specific and competitive antagonist of GLP-1R (19). Exendin-(9-39) was originally described as a weak partial agonist (15,20) and was later shown to be a neutral antagonist (21) and inverse agonist (19) in different model systems. Regardless, exendin-(9-39) (generic name, avexitide) has been shown to be an effective GLP-1R antagonist that has been tested as a potential treatment for both HI and acquired hyperinsulinemic hypoglycemia secondary to bariatric surgery (14,22–24). Previous studies have shown that exendin-(9-39) suppresses insulin secretion and corrects fasting hypoglycemia in *Sur1*$^{-/-}$ mice without affecting glucose tolerance or insulin sensitivity (13). In a pilot clinical study of nine adolescents and adults with K_{ATP}-HI, fasting plasma glucose level was significantly increased and insulin to glucose ratios were significantly lower with exendin-(9-39) treatment (14). In addition, exendin-(9-39) significantly inhibited amino acid–stimulated insulin secretion in pancreatic islets isolated from neonates with K_{ATP}-HI (14). In a more recent study, treatment with exendin-(9-39) significantly prevented fasting and protein-induced hypoglycemia in children with K_{ATP}-HI (22). A limitation of exendin-(9-39) is its short serum half-life that would require multiple daily doses (25,26).

Previously, we described the development of a GLP-1R antagonist antibody, TB-001-003 (27). TB-001-003 has a unique complementary determining region 3 of the heavy chain (HCDR3) that is an elongated loop with a grafted fragment of GLP-1. We previously characterized the discovery of TB-001-003 from phage panning on GLP-1R–overexpressing cells. Our GPCR-focused phage display library contains grafted peptides from known GPCR ligands in the HCDR3, along with random variations. The other complementary determining regions (CDRs) are taken from the naturally occurring repertoire of CDRs in the human genome. Using high-quality, silicon-based oligonucleotide DNA synthesis, we were able to construct a library of $>10^{10}$ phage display single-chain variable fragments with a high likelihood of binding to GPCRs. After reformatting the single-chain variable fragments from enriched phage into full-length antibodies, we characterized the binding and pharmacology of our GPCR-targeted antibodies for further development.

Here, we wanted to optimize the previously characterized antagonist activity of TB-001-003. To do that, we implemented a novel antibody optimization algorithm, called Twist Antibody Optimization (TAO). For TB-001-003, we made 444 mutations to the HCDR3 containing a fragment of the GLP-1 peptide and combined them with naturally occurring CDRs from the human repertoire to generate a library of $>10^{13}$ phage. After panning and reformatting, we discovered an optimized antibody antagonist, TB-222-023, as well as two partial agonists, TB-222-040 and TB-222-089. TB-222-023 was an ∼10-fold more potent antagonist than exendin-(9-39) and had no partial agonism at G protein or β-arrestin 2 activation (and even displayed inverse agonism for β-arrestin 2 recruitment).

As the exendin-(9-39) published data demonstrate, antagonism of GLP-1R is a viable treatment for HI. Using the *Sur1*$^{-/-}$ mouse model and islets from an infant with HI, we evaluated the effect of GLP-1R antagonism by GLP-1R–directed antibodies in the context of hyperinsulinism. TB-222-023 showed remarkable amelioration of hypoglycemia in the *Sur1*$^{-/-}$ mouse model of hyperinsulinism and significant reduction of insulin secretion in pancreatic islets isolated from an infant with HI. Taken together, we show that an antibody antagonist targeted against GLP-1R has a superior antagonist profile in vitro and is highly effective in vivo.

RESEARCH DESIGN AND METHODS

TAO Algorithm and Library Design

The CDRs from the IGHV3-30/33 germline variable heavy chains and IGLV1–51 variable light chains were synthesized by Twist Bioscience in oligo pools, along with the

CDR3 identified by Liu et al. (27) with 433 point mutations for a total library of 3.35×10^{13} single-chain variable fragments grafted into phagemids.

Cell-Based Phage Panning

Phage panning was performed as previously described (27) with one exception: the antagonist antibody TB-001-003 was added to the phage in molar excess to bias the population toward high-affinity binders.

Animals

All studies were conducted at the Children's Hospital of Philadelphia, and the Institutional Animal Care and Use Committee approved all procedures.

Sur1$^{-/-}$ male mice with a C57BL/6J genetic background were bred via *Sur1*$^{-/-}$ male by *Sur1*$^{-/-}$ female crosses and maintained in our animal facility. The generation of *Sur1*$^{-/-}$ mice was previously described (7). Wild-type (WT) (C57Bl/6J) control male mice were acquired from The Jackson Laboratory. Male, 12–18-week-old *Sur1*$^{-/-}$ and WT mice were maintained on a 12/12-h light/dark cycle and were fed a standard rodent chow diet.

Fasting Evaluation

Four doses of either vehicle (100 mmol/L HEPES, 100 mmol/L NaCl, 50 mmol/L NaOAC, pH 6.0), TB-001-003 (30 mg/kg), or TB-222-023 (30 mg/kg) were administered to *Sur1*$^{-/-}$ or WT male mice (n = 7 per group) by intraperitoneal injections over 2 weeks. Fasting (16 h overnight) plasma glucose level was assessed 7 days before the first dose and the day after each dose. Fasting (16 h overnight) insulin and β-hydroxybutyrate levels were assessed at baseline 7 days before the first dose and the day after the second and fourth doses.

Glucose Tolerance Test

An intraperitoneal glucose tolerance test (IPGTT) was completed the day after the final dose on day 12. After overnight fasting after the fourth dose, mice were injected with glucose (2 g/kg), and then plasma glucose level was evaluated every 30 min for 2 h. Plasma insulin was evaluated at 0, 30, and 60 min after glucose injection and measured by ELISA (Mouse Ultrasensitive Insulin ELISA; catalog 80-INSMSU-E10, ALPCO).

Pancreatic Islet Culture

Human HI islets were isolated from fresh pancreata from surgical specimens from neonates procured through an institutional review board–approved protocol at the Congenital Hyperinsulinism Center at the Children's Hospital of Philadelphia. Pancreas tissue was injected with collagenase (0.75% collagenase P; Roche, catalog 11249002001) and digested at 37°C. Human islets were hand-picked by microscopy and cultured in completed PIM(S) medium (PIM-S; PRODO Laboratory) with 5 mmol/L glucose for 2–3 days.

Mouse pancreatic tissue was digested in 0.75% collagenase P (catalog 11249002001, Roche) at 37°C; islets were hand-picked by microscopy and then cultured for 2–3 days in RPMI 1640 medium (Sigma, catalog R1383) with 10 mmol/L glucose. RPMI 1640 medium was supplemented with 23.8 mmol/L $NaHCO_3$, 10% FBS, 2 mmol/L glutamine, 100 units/mL penicillin, and 50 mg/mL streptomycin. All islets were cultured at 37°C in a 5% CO_2, 95% air-humidified incubator.

Static Batch Incubation

Five primary isolated pancreatic WT mouse islets (n = 8 replicates) were picked per well. Islets were untreated or preincubated with either 100 nmol/L or 1 μmol/L TB-001-003 or TB-222-023 for 1 h at 37°C in a cell culture incubator. Islets were then stimulated with 3, 10, or 25 mmol/L glucose for 90 min. Secreted insulin was assessed by homogenous time-resolved fluorescence assay.

Pancreatic Islet Perifusion

Islets were untreated or treated with TB-001-003 (500 nmol/L) or TB-222-023 (500 nmol/L). Batches of 300 cultured islets were loaded onto a nylon filter in a chamber. Perfusion was performed in Krebs–Ringer bicarbonate buffer (115 mmol/L NaCl, 24 mmol/L $NaHCO_3$, 5 mmol/L KCl, 1 mmol/L $MgCl_2$, 2.5 mmol/L $CaCl_2$, 10 mmol/L HEPES, pH 7.4) with 0.25% BSA at 37°C. Islets were stimulated with 3 mmol/L glucose and amino acid mixture (AAM) ramp (0–12 mmol/L) followed by KCl (60 mmol/L). The mixing of 19 amino acids was previously described (8). Fractions were collected at a rate of 1 mL/min. Secreted insulin was measured by homogenous time-resolved fluorescence assay (CisBio, catalog 621N1PEH) and read on a compatible plate reader (CLARIOstar; BMG LABTECH).

Cross-reactivity Analysis

For receptor cross-reactivity of TB-001-003 and TB-222-023, green fluorescent protein–tagged class B1 GPCRs were ordered from Origene (VIPR2: RG203761; SCTR: RG207786; CT RG210171; gastric inhibitory polypeptide receptor [GIPR]: RG210811; PTH2R: RG210906; GLR: RG211179; CALRL: RG212215; PTH1R: RG212841; PACR: RG215923; GLP-2R: RG220745; CRFR2: RG222881; CRFR1: RG226816). The receptors were expressed in Expi293T cells and binding was carried out as described above. In addition, control antibodies were purchased from Origene (PTH2R: AP02242SU-N; CRFR2: AP51079PU-N; PACR: TA324123) and R&D (CALRL: MAB10044-SP; GLR: MAB10296-SP; CRFR1: MAB3930-SP; GLP-2R: MAB4285-SP; VPAC2: MAB5416-SP; PTH1R: MAB5709-SP; SCTR: MAB6387-SP; GIPR: MAB8-210-SP). Fluorescence levels of green fluorescent protein were normalized to untransfected cells to calculate the relative level of total receptor expression. Control antibodies were normalized to untransfected cell binding to calculate the surface level of receptor expression. Relative binding of TB-001-003 and TB-222-023 was normalized to binding to untransfected cells.

Statistical Methods

Statistical analyses were performed with GraphPad Prism software, version 9. Results are presented as mean ± SEM. The level of significance was set at $P < 0.05$. For multiple measurements, data were analyzed using two-way repeated measures ANOVA and Tukey multiple comparison test. Single-time end-point data were analyzed using a single-factor ANOVA test.

Data and Resource Availability

All data generated or analyzed during this study are included in the published article (and its online supplementary files). No applicable resources were generated or analyzed during this study.

RESULTS

Antibody Optimization for Improved GLP-1R Antagonism

Our goal was to generate improved GLP-1R antagonist antibodies based on our previously described antibody, TB-001-003. To achieve this goal, phage display on cells overexpressing GLP-1R was performed (Fig. 1*A*). In addition, full-length TB-001-003 was added during the GLP-1R binding step to bias the phage clone population toward more potent binders. Twist DNA synthesis infrastructure was used to synthesize a combinatorial library of CDR variants, including mutagenesis of the heavy CDR3 (HCDR3) of TB-001-003 and an optimized library of the five other CDRs (Fig. 1*B*). TB-001-003 has an HCDR3 that mimics the α helix of GLP-1R ligands (Supplementary Fig. 1*A* and *B*). Phage enrichment was observed after three rounds of panning, and each round had more stringent washes as well as less available antigen (Fig. 1*C*). A total of 94 phage clones were reformatted into full-length IgG antibodies and purified with Protein A packed pipette tips using the Twist high-throughput IgG platform.

The 94 clones were tested for activation of cAMP (Fig. 2*A*), antagonism (Fig. 2*B*), and binding (Fig. 2*C*) at a single-point concentration after pH neutralization. Surprisingly, two clones, TB-222-040 and TB-222-089, showed weak partial agonism at GLP-1R for cAMP accumulation (Fig. 2*A*). TB-222-040 and TB-222-089 have a point mutation in the GLP-1 ligand-like HCDR3 (E21L and R36D, respectively, using GLP-1 amino acid numbering; Supplementary Fig. 1*B*). In total, 11 clones had binding and antagonism profiles that matched or improved upon TB-001-003. Otherwise, the other clones had a mixed effect on reducing binding, antagonism, or both (Fig. 2*D*).

Discovery of Novel GLP-1R Antagonists With Complex Pharmacology

Next, to fully evaluate the two top antagonists (TB-001-003 and TB-222-023) and the two partial agonists (TB-222-040 and TB-222-089) for binding, G protein activity, and β-arrestin 2 recruitment. For β-arrestin 2 recruitment, we used split nanoluc complementation and saw robust and potent exendin-4–stimulated recruitment (Supplementary Fig. 2*A*). For G protein activation, we used the GloSensor (Promega) biosensor and saw robust and potent activation with known GLP-1R agonists (Supplementary Fig. 2*B*). TB-001-003 and

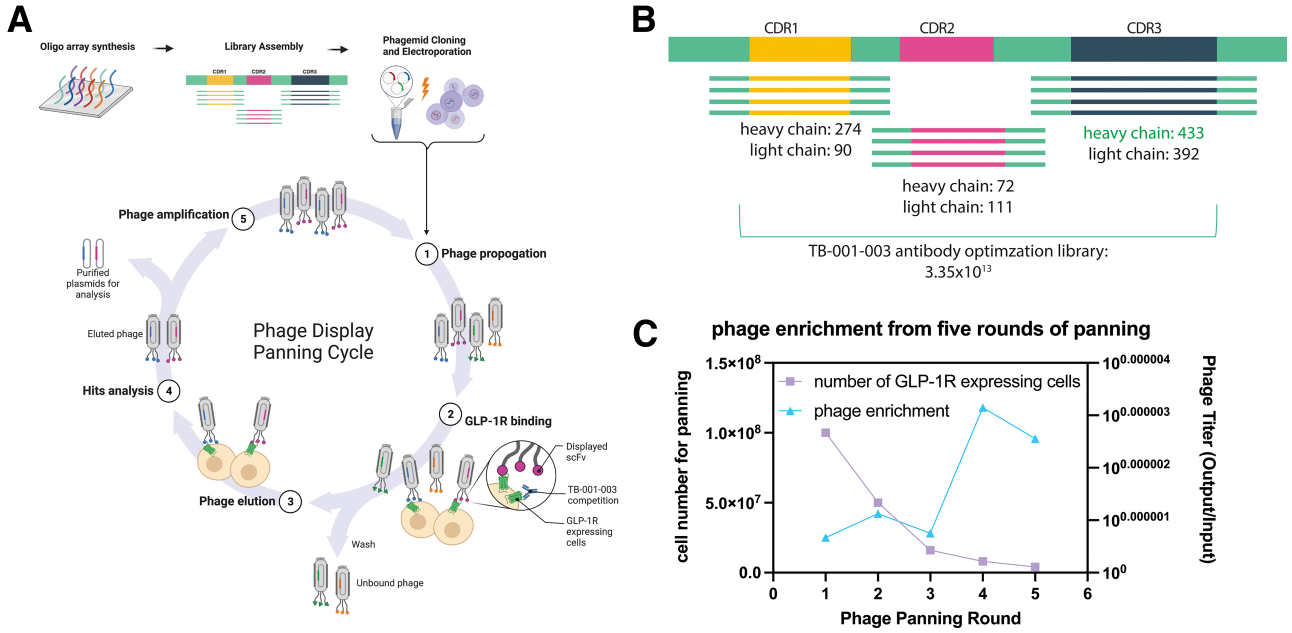

Figure 1—Panning strategy for antibody optimization. *A*: DNA libraries synthesized in house were electroporated into phage and panned in five successive rounds against GLP-1R-expressing cells. *B*: Library design, based on TB-001-003. HCDR3 sequence was mutagenized into 433 different variations; other CDRs were taken from naturally occurring human repertoire to yield 3.35×10^{13} antibodies. *C*: Enrichment of phage after five rounds of panning with increased washing stringency and lowered available antigen by decreasing cell number.

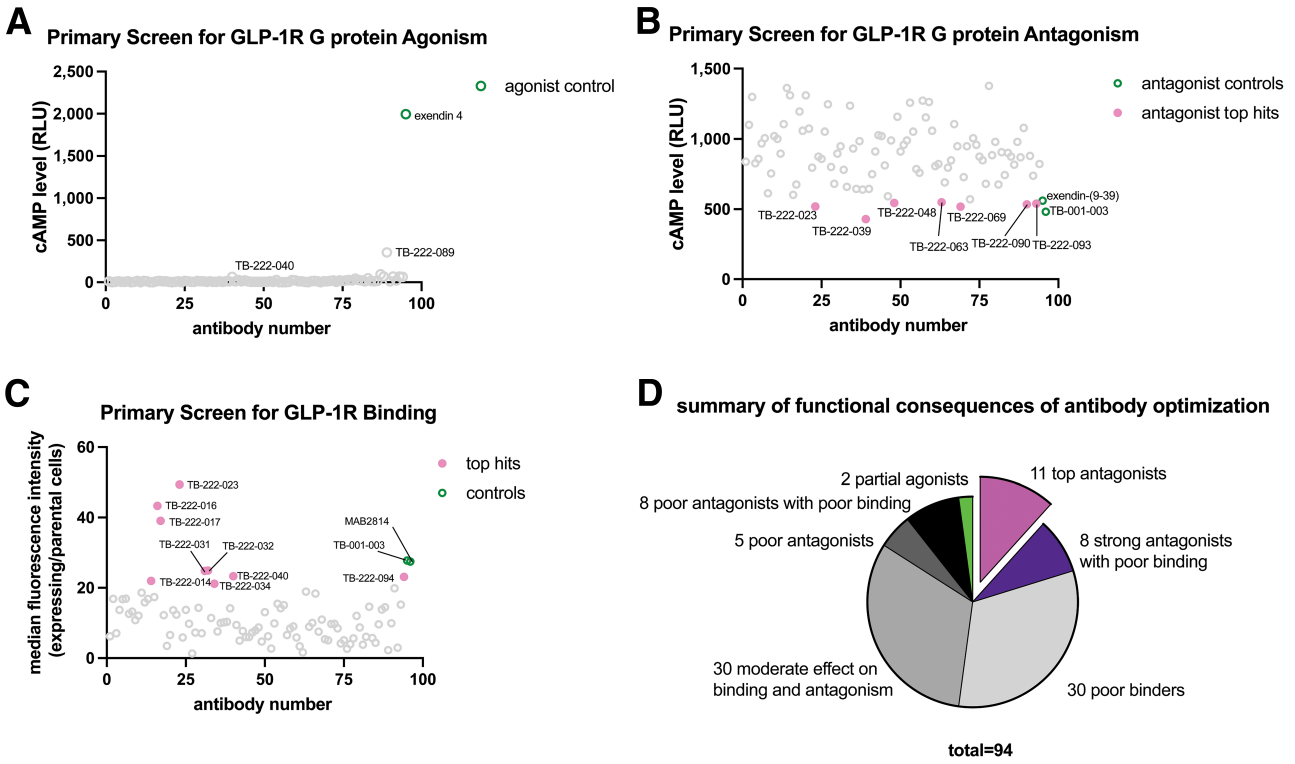

Figure 2—Primary screen of top 94 phage clones for binding, G protein agonism and antagonism. *A*: Primary agonist screen reveals two potential partial agonists, TB-222-040 and TB-222-089. *B*: Primary G protein–antagonist screen reveals seven antagonists with strong efficacy. *C*: Primary screen of single-point binding reveals nine clones with enhanced GLP-1R binding by flow cytometry. *D*: Summary of each antibody screened.

TB-222-023 bound well to GLP-1R–expressing cells, as assessed by flow cytometry (Fig. 3*A*). Cells expressing high levels of GLP-1R correlated with high antibody binding (Fig. 3*B*) and both antibodies bound with nanomolar potency (Fig. 3*C* and Supplementary Table 1). TB-222-040 and TB-222-089 had similar robust GLP-1R binding profiles (Supplementary Fig. 3*A*–*C* and Supplementary Table 1).

When evaluated for agonism and antagonism, TB-222-040 and TB-222-089 showed an interesting profile. Like exendin-(9-39), TB-222-040 showed weak activation of cAMP accumulation over background (with an E_{MAX} of less than 2% of exendin-4) (Fig. 3*D* and Supplementary Table 1). Interestingly, TB-222-089 displayed even less G protein activation but was able to elicit a weak β-arrestin 2 response (Supplementary Fig. 3*E*). TB-222-040 and TB-222-089 were poor antagonists at both the G protein and β-arrestin 2 pathways, which is a hallmark of partial agonism (28).

In contrast, TB-001-003 and TB-222-023 reduced the basal β-arrestin 2 recruitment level (Fig. 3*E*) which is typical of inverse agonists. However, this was not seen at the G protein pathway (Supplementary Fig. 3*D*). GLP-1R has recently been described as having little constitutive G protein activity when overexpressed in heterologous cells (29,30). TB-001-003 and TB-222-023 were potent antagonists at the GLP-1R G protein pathway (Fig. 3*F*), beating exendin-(9-39) potency by ∼10-fold (Supplementary Table 1). In addition, TB-001-003 and TB-222-023 were more potent than exendin(9-39) when challenged with five different GLP-1R agonists (Supplementary Fig. 2*C*–*G*) while the commercially available GLP-1R antibody (MAB2814) showed only weak GLP-1R inhibition. Glucagon is another GLP-1R agonist (31) and was also blocked by both antibodies to a higher degree than exendin-(9-39) (Supplementary Fig. 2*G*). TB-222-023 indeed showed a slight enhancement of antagonist potency over TB-001-003. In contrast, the β-arrestin 2 antagonism was equipotent among TB-001-003, TB-222-023, and exendin-(9-39) (Fig. 3*G*). These data demonstrate that the antibody optimization campaign yielded antagonist antibodies with unique pharmacology: partial agonists, inverse agonists, and antagonists with biased GPCR signaling–inhibition profiles.

Treatment of Hyperinsulinism with GLP-1R Antibody Antagonists

To assess the effect of GLP-1R antagonist antibodies TB-001-003 and TB-222-023 on plasma glucose in vivo, we administered four doses by intraperitoneal injection over 12 days to WT mice and also *Sur1*$^{-/-}$ mice, a mouse model of K_{ATP}-HI. In WT mice treated with TB-001-003 or TB-222-023 (Fig. 4*A*), we observed a trend of increased fasting plasma glucose levels compared with vehicle-treated control mice, with a statistically significant increase after the first and third doses. Treatment of WT mice with TB-001-003 or TB-222-023 showed a decreasing trend in

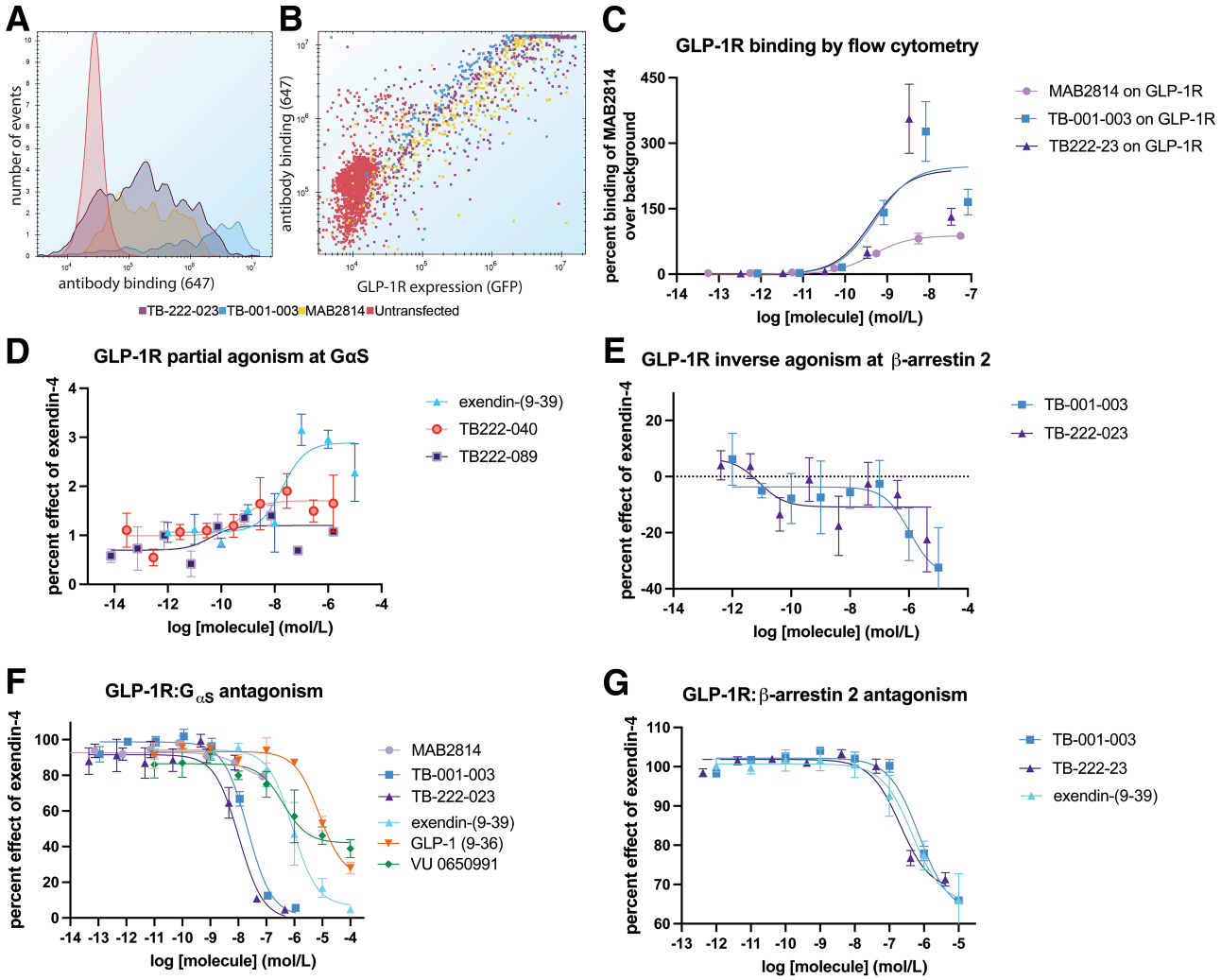

Figure 3—Pharmacological characterization of top agonists and antagonists. *A*: Histogram of antibodies binding to GLP-1R. *B*: Scatter overlay showing antibody binding relative to GLP-1R expression. *C*: Determination of half-maximal effective concentration binding to GLP-1R–expressing cells. *D*: TB-222-040 and TB-222-089 show weak partial activity at cAMP accumulation. *E*: TB-001-003 and TB-222-023 decrease basal β-arrestin 2 recruitment to GLP-1R. *F*: TB-001-003 and TB-222-023 are highly potent GLP-1R G protein antagonists. *G*: TB-001-003 and TB-222-023 block β-arrestin 2 recruitment to a similar level as exendin-(9-39).

plasma insulin levels, a significantly lower insulin to glucose ratio after the second dose of TB-222-023, and no change in β-hydroxybutyrate (Supplementary Fig. 4*A*–*C*). Fasting plasma glucose level is significantly increased in *Sur1*$^{-/-}$ mice treated with TB-001-003 after each of the four doses compared with vehicle controls (Fig. 4*B*). With TB-222-023 treatment, a significant increase in plasma glucose level was observed after the first and fourth doses in *Sur1*$^{-/-}$ mice (Fig. 4*B*). Importantly, we found that fasting plasma glucose level in *Sur1*$^{-/-}$ mice after the fourth injection of either TB-001-003 or TB-222-023 is similar to that of vehicle-treated WT mice (compare Fig. 4*A* and Fig. 4*B*). Both antibodies are able to normalize the fasting plasma glucose level and prevent fasting hypoglycemia in *Sur1*$^{-/-}$ mice. Compared with vehicle controls, plasma insulin and β-hydroxybutyrate levels are not significantly decreased in *Sur1*$^{-/-}$ mice treated with TB-001-003 or TB-222-023, but the insulin to glucose ratio is significantly decreased after the fourth dose of both antibodies (Supplementary Fig. 4*D*–*F*). Evaluation by IPGTT demonstrated that the glucose excursion in response to a glucose load was not significantly higher in WT mice treated with TB-001-003 but is significantly higher with TB-222-023 treatment compared with vehicle controls (Fig. 4*C*–*D*). Plasma insulin or the insulin to glucose ratio was not significantly changed with treatment of TB-001-003 or TB-222-023 at baseline (0 min), 30, or 60 min after the administration of glucose in WT mice compared with vehicle control (Supplementary Fig. 4*G* and *H*). IPGTT of *Sur1*$^{-/-}$ mice revealed that glucose excursion in response to a glucose load was significantly higher with treatment with either TB-001-003 and TB-222-023 compared with vehicle controls (Fig. 4*E*–*F*). Although plasma insulin was not significantly changed in *Sur1*$^{-/-}$ mice treated with TB-001-003 or TB-222-023 during the 0-, 30-, or 60-min time points of

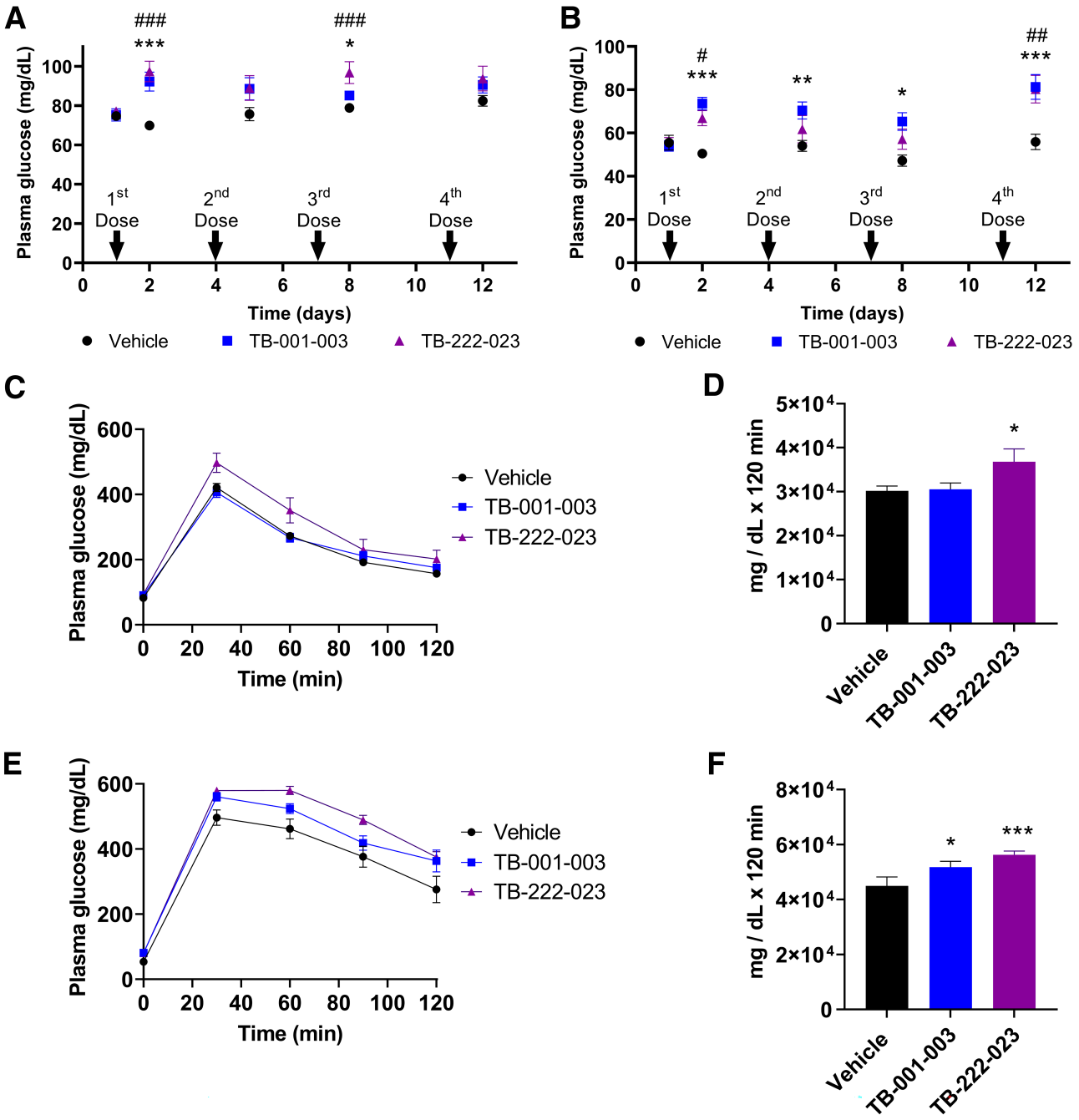

Figure 4—TB-001-003 and TB-222-023 effectually increase plasma glucose in WT and *Sur1*$^{-/-}$ mice. *A* and *B*: A fasting evaluation was completed in (*A*) WT and (*B*) *Sur1*$^{-/-}$ mice. *C*: GTT results in WT mice treated with TB-001-003 and TB-222-023. *D*: Area under the curve (AUC) calculation of WT TB-001-003 and TB-222-023 GTT. *E*: GTT in TB-001-003 and TB-222-023 treated *Sur1*$^{-/-}$ mice. *F*: AUC calculation for *Sur1*$^{-/-}$ TB-001-003 and TB-222-023 GTT. Error bars represent ± SEM. Statistics calculated using single-factor ANOVA. $n = 7$. For *A* and *B* compared with vehicle control, symbols * for TB-001-003 and # for TB-222-023 used. * or #$P < 0.05$, ** or ##$P < 0.01$, *** or ###$P < 0.001$. For *D* and *F* compared with vehicle control, *$P < 0.05$, **$P < 0.01$, ***$P < 0.001$.

the IPGTT, a significant decrease in the insulin to glucose ratio was observed at baseline (0 min) with treatment with both TB-001-003 and TB-222-023 (Supplementary Fig. 4*I* and *J*).

Subsequently, we evaluated the effect of TB-001-003 or TB-222-023 on insulin secretion dynamics. To ascertain an effective concentration in vitro, we completed a static batch incubation of WT mouse islets with glucose and compared total insulin secretion with no treatment to that with two different treatment doses of TB-001-003 or TB-222-023 treatment (100 nmol/L and 1 μmol/L). We observed a significant reduction of total insulin secretion at all glucose concentrations (3, 10, and 25 mmol/L) with a 1 μmol/L concentration of either TB-001-003 or TB-222-023

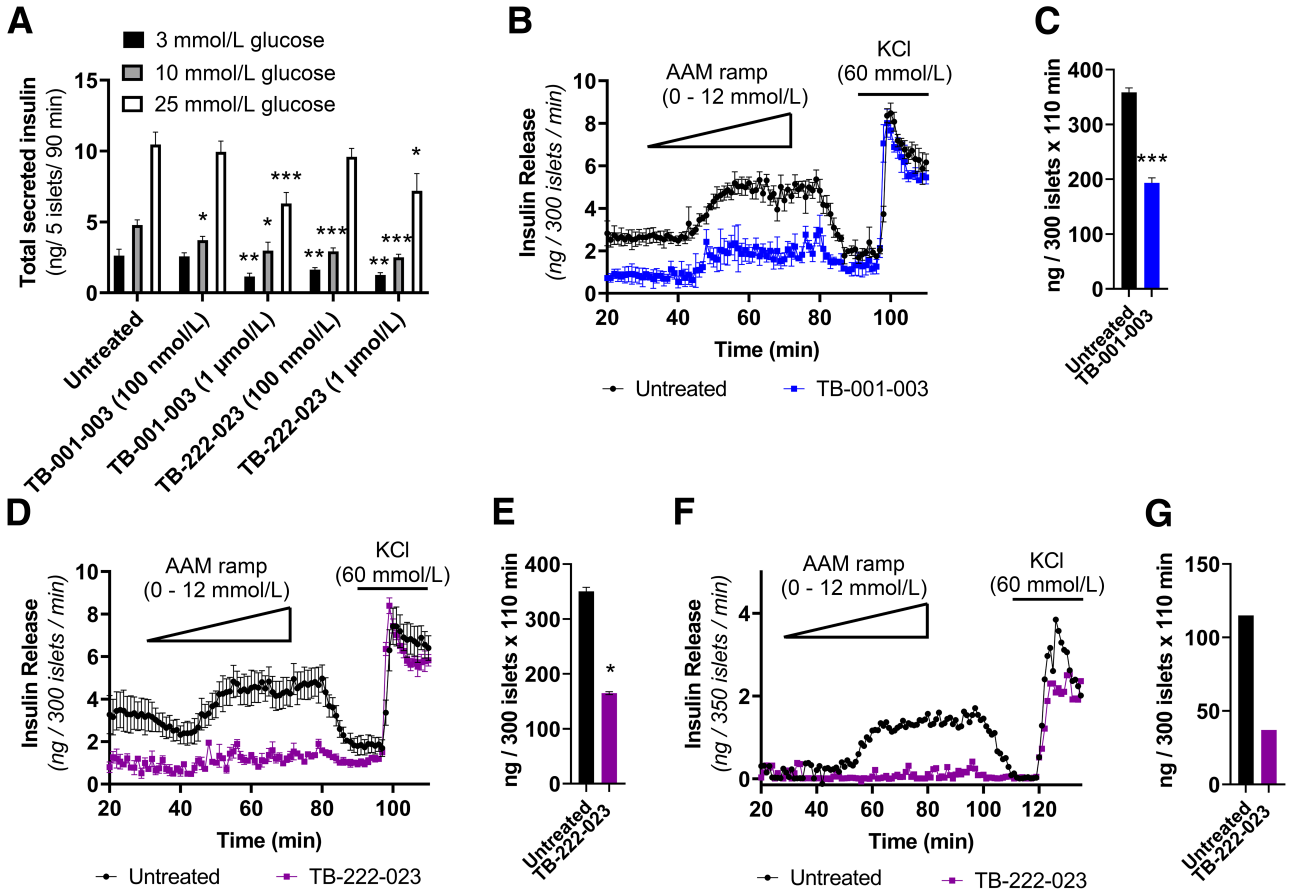

Figure 5—TB-001-003 and TB-222-023 significantly decrease insulin secretion in mouse and human pancreatic islets from pancreas with high insulin. *A*: Static batch incubation of WT mouse islets with denoted glucose concentrations with no treatment or with TB-001-003 or TB-222-023. *B*: Perifusion of *Sur1*$^{-/-}$ mouse islets with 3 mmol/L glucose and a physiologic AAM ramp (0–12 mmol/L) followed by KCl with or without TB-001-003 (500 nmol/L). *C*: Area under the curve (AUC) calculation of TB-001-003 perifusion. *D*: Perifusion of *Sur1*$^{-/-}$ mouse islets with 3 mmol/L glucose and a physiologic AAM ramp (0 to 12 mmol/L) followed by KCl with or without TB-222-023 (500 nmol/L). *E*: AUC calculation of TB-222-023 perifusion. *F*: Perifusion of islets isolated from an infant with K_{ATP}-HI treated with or without TB-222-023. *G*: AUC calculation of human HI islet perifusion. All GLP-1R antibody treatments by perifusion were significantly different from controls by two-way ANOVA ($P < 0.0001$). Error bars represent ± SEM. Batch incubation and AUC statistics were calculated using single-factor ANOVA. *$P < 0.05$, **$P < 0.01$, ***$P < 0.001$.

(Fig. 5*A*). Results demonstrated that TB-001-003 and TB-222-023 are able to significantly abrogate insulin secretion in response to a physiologic AAM in *Sur1*$^{-/-}$ islets (Fig. 5*B–E*). Encouraged by the significant decrease in insulin secretion in *Sur1*$^{-/-}$ islets, we next evaluated the effect of GLP-1R antagonism in human islets isolated from a patient diagnosed with HI who required pancreatectomy for intractable hypoglycemia. We conducted a perifusion with an AAM ramp on islets from an infant with K_{ATP}-HI caused by an inactivating, pathogenic dominant mutation in *ABCC8* (c.4157C>T). Treatment with TB-222-023 significantly reduced AAM-stimulated insulin secretion in these human K_{ATP}-HI islets compared with untreated control islets (Fig. 5*F* and *G*). Importantly, our results demonstrate the ability of GLP-1R antagonism via directed antibodies to decrease insulin secretion in both islets from the *Sur1*$^{-/-}$ mouse model of K_{ATP}-HI and in human K_{ATP}-HI islets.

DISCUSSION

Antibody treatments have become increasingly prevalent and hold great potential because they have fewer side effects and a longer half-life compared with other therapies (32). Here, we describe the development of novel anti–GLP-1R antibodies that function as potent and specific (Supplementary Fig. 5) antagonists. GLP-1R has been targeted by peptide agonists in the clinic for the treatment of obesity and type 2 diabetes (33). Therefore, many studies have elucidated the function of natural and synthetic GLP-1R agonists (34). Briefly, GLP-1R activation occurs through binding of ligands in the orthosteric binding site found on most GPCRs. GLP-1R is a member of the class B family of secretin GPCRs, which all contain a unique large N-terminal domain that also participates in ligand binding and signal transduction (31,35). Exendin-(9-39) has its N terminus proteolyzed, which means the orthosteric binding site is no longer intact. Similarly, the TB-222

series of antibodies seem to only bind to the N-terminal binding site (Supplementary Fig. 1*A*). It is interesting to note that exendin-(9-39), TB-222-040, and TB-222-089 are able to elicit partial agonism of GLP-1R through interactions mostly with the N-terminal domain. This N-terminal domain activation is reminiscent of the recently described synthetic GLP-1R agonist (36) that seems to bind to extracellular loops of GLP-1R and transmits activation through coordination of the receptor's polar core and structural water molecules.

It has been suggested that exendin-(9-39) is an inverse agonist of GLP-1R (19,37). Although both antagonists and inverse agonists can have an effect on receptor activity in the presence of agonist, a defining characteristic of an inverse agonist is the ability to have an effect in the absence of agonist. Our experimental data indicate that the GLP-1R antibodies TB-001-003 and TB-222-023 may also be inverse agonists. We see a significant decrease in the basal levels of insulin secretion with TB-001-003 or TB-222-023 treatment when no secretagogue (glucose or AAM) is present during batch incubation and perifusion experiments of isolated islets (Fig. 5). In our data, we observed neutral antagonism at the G protein pathway (Fig. 3*F*) but inverse agonism at the β-arrestin 2 pathway (Fig. 3*E*). Taken together with the slight partial agonism at the G protein and β-arrestin 2 pathways of exendin-(9-39) seen in Fig. 2*D* and Supplementary Fig. 3*E*, respectively, it is clear that our antibody antagonists have a very different pharmacology at GLP-1R. This inverse agonism we observed in vitro at β-arrestin 2 recruitment seems to be predictive of the in vivo inverse agonism we observed for TB-001-003 and TB-222-023 and may be critical for a new GLP-1R mechanism of insulin regulation.

The recently approved GLP-1R/GIPR dual agonist tirzepatide shows a unique G protein–biased profile at GLP-1R (38). Interestingly, tirzepatide was recently shown to exert a different orientation of the N-terminal domain when bound to GLP-1R, compared with GLP-1 binding (39). As we observed with TB-222-040 and TB-222-089, there seems to be biased partial activation of G protein or β-arrestin 2 pathways, respectively. GLP-1R signaling through G proteins and β-arrestin pathways has been very well elucidated, with a number of potent ligands identified that signal through GLP-1R's pleiotropic pathways (35,40). Therefore, TB-222 partial agonists show that some of that bias is directed through N-terminal domain interactions.

The GLP-1R has been shown to be a promising target to treat congenital and acquired forms of hyperinsulinemic hypoglycemia that may offer some advantages over currently available treatments (14,22–25). The approach so far has been centered on the use of exendin-(9-39) peptide, which has a short half-life (25,26). GLP-1R antagonism via targeted antibodies such as TB-001-003 and TB-222-023 offer great potential in this regard because they demonstrate a much longer half-life, which would require less frequent dosing and, therefore, ease of treatment for patients. Antibody therapeutics have many advantages over peptides, and antibodies can be engineered to avoid toxic effector functions, including antibody-dependent cellular cytotoxicity (41). Antibodies are processed through intracellular recycling (42), and antibody half-life can be enhanced through engineering of the crystallizable fragment region (43). Finally, antibodies tend to accumulate in tissues that have high expression of target receptors, as was demonstrated for an anti-GIPR antibody that accumulated in the pancreas (44). Here, we have shown that GLP-1R antagonist antibodies such as TB-222-023 are potential applicable treatments for patients with K_{ATP}-HI in whom diazoxide is commonly unsuccessful (Fig. 5*F* and *G*).

TB-222-023 is a unique GLP-1R antagonist that shows a marked improvement over exendin-(9-39) antagonism. Here, we demonstrate in vivo efficacy for the treatment of HI. TB-222-023 is a full-length antibody with likely significantly superior serum half-life (27), more potent GLP-1R blocking in the pancreas compared with current available treatments, and the potential to improve treatment regimens and outcomes for patients with HI.

Duality of Interest. S.M.P., C.F.H., C.H., A.G.L.H., Z.C., L.W., Z.H., N.H., R.S., F.A., T.Z.Y., and A.K.S. are employees of and own stock in Twist Bioscience. Twist Bioscience provided funding for this study. No other potential conflicts of interest relevant to this article were reported.

Author Contributions. S.M.P. and C.A.J. conducted experiments, analyzed data, and wrote the manuscript. C.F.H. and J.C. conducted experiments, reviewed and edited the manuscript. C.H., K.Y.C., A.G.L.H., L.W., and T.Z.Y. conducted experiments and analyzed data. Z.C., Z.H., N.H., R.S., and F.A. analyzed data and reviewed the manuscript. D.D.D.L. and A.K.S. are responsible for the overall design and conduction of the study and reviewed/edited the manuscript. D.D.D.L. and A.K.S. are the guarantors of this work and, as such, had full access to all the data in the study and take responsibility for the integrity of the data and the accuracy of the data analysis.

References

1. Stanley CA. Advances in diagnosis and treatment of hyperinsulinism in infants and children. J Clin Endocrinol Metab 2002;87:4857–4859

2. Lord K, Dzata E, Snider KE, Gallagher PR, De León DD. Clinical presentation and management of children with diffuse and focal hyperinsulinism: a review of 223 cases. J Clin Endocrinol Metab 2013;98:E1786–E1789

3. Seino S, Miki T. Physiological and pathophysiological roles of ATP-sensitive K+ channels. Prog Biophys Mol Biol 2003;81:133–176

4. Dunne MJ, Cosgrove KE, Shepherd RM, Aynsley-Green A, Lindley KJ. Hyperinsulinism in infancy: from basic science to clinical disease. Physiol Rev 2004;84:239–275

5. Beltrand J, Caquard M, Arnoux JB, et al. Glucose metabolism in 105 children and adolescents after pancreatectomy for congenital hyperinsulinism. Diabetes Care 2012;35:198–203

6. Lord K, Radcliffe J, Gallagher PR, Adzick NS, Stanley CA, De León DD. High risk of diabetes and neurobehavioral deficits in individuals with surgically treated hyperinsulinism. J Clin Endocrinol Metab 2015;100:4133–4139

7. Seghers V, Nakazaki M, DeMayo F, Aguilar-Bryan L, Bryan J. Sur1 knockout mice. A model for K(ATP) channel-independent regulation of insulin secretion. J Biol Chem 2000;275:9270–9277

8. Shiota C, Larsson O, Shelton KD, et al. Sulfonylurea receptor type 1 knock-out mice have intact feeding-stimulated insulin secretion despite marked impairment in their response to glucose. J Biol Chem 2002;277:37176–37183

9. Li C, Buettger C, Kwagh J, et al. A signaling role of glutamine in insulin secretion. J Biol Chem 2004;279:13393–13401
10. Doliba NM, Wehrli SL, Vatamaniuk MZ, et al. Metabolic and ionic coupling factors in amino acid-stimulated insulin release in pancreatic beta-HC9 cells. Am J Physiol Endocrinol Metab 2007;292:E1507–E1519
11. Fourtner SH, Stanley CA, Kelly A. Protein-sensitive hypoglycemia without leucine sensitivity in hyperinsulinism caused by K(ATP) channel mutations. J Pediatr 2006;149:47–52
12. Hsu BY, Kelly A, Thornton PS, Greenberg CR, Dilling LA, Stanley CA. Protein-sensitive and fasting hypoglycemia in children with the hyperinsulinism/hyperammonemia syndrome. J Pediatr 2001;138:383–389
13. De León DD, Li C, Delson MI, Matschinsky FM, Stanley CA, Stoffers DA. Exendin-(9-39) corrects fasting hypoglycemia in SUR-$1^{-/-}$ mice by lowering cAMP in pancreatic beta-cells and inhibiting insulin secretion. J Biol Chem 2008;283:25786–25793
14. Calabria AC, Li C, Gallagher PR, Stanley CA, De León DD. GLP-1 receptor antagonist exendin-(9-39) elevates fasting blood glucose levels in congenital hyperinsulinism owing to inactivating mutations in the ATP-sensitive K+ channel. Diabetes 2012;61:2585–2591
15. Raufman JP, Singh L, Eng J. Exendin-3, a novel peptide from *Heloderma horridum* venom, interacts with vasoactive intestinal peptide receptors and a newly described receptor on dispersed acini from guinea pig pancreas. Description of exendin-3(9-39) amide, a specific exendin receptor antagonist. J Biol Chem 1991;266:2897–2902
16. Chan HCS, Li Y, Dahoun T, Vogel H, Yuan S. New binding sites, new opportunities for GPCR drug discovery. Trends Biochem Sci 2019;44:312–330
17. Zhang Y, Sun B, Feng D, et al. Cryo-EM structure of the activated GLP-1 receptor in complex with a G protein. Nature 2017;546:248–253
18. Montrose-Rafizadeh C, Yang H, Rodgers BD, Beday A, Pritchette LA, Eng J. High potency antagonists of the pancreatic glucagon-like peptide-1 receptor. J Biol Chem 1997;272:21201–21206
19. Serre V, Dolci W, Schaerer E, et al. Exendin-(9-39) is an inverse agonist of the murine glucagon-like peptide-1 receptor: implications for basal intracellular cyclic adenosine 3′,5′-monophosphate levels and beta-cell glucose competence. Endocrinology 1998;139:4448–4454
20. Göke R, Fehmann HC, Linn T, et al. Exendin-4 is a high potency agonist and truncated exendin-(9-39)-amide an antagonist at the glucagon-like peptide 1-(7-36)-amide receptor of insulin-secreting beta-cells. J Biol Chem 1993;268:19650–19655
21. Thorens B, Porret A, Bühler L, Deng SP, Morel P, Widmann C. Cloning and functional expression of the human islet GLP-1 receptor. Demonstration that exendin-4 is an agonist and exendin-(9-39) an antagonist of the receptor. Diabetes 1993;42:1678–1682
22. Stefanovski D, Vajravelu ME, Givler S, De León DD. Exendin-(9-39) effects on glucose and insulin in children with congenital hyperinsulinism during fasting and during a meal and a protein challenge. Diabetes Care 2022;45:1381–1390
23. Craig CM, Lawler HM, Lee CJE, et al. PREVENT: a randomized, placebo-controlled crossover trial of avexitide for treatment of postbariatric hypoglycemia. J Clin Endocrinol Metab 2021;106:e3235–e3248
24. Tan M, Lamendola C, Luong R, McLaughlin T, Craig C. Safety, efficacy and pharmacokinetics of repeat subcutaneous dosing of avexitide (exendin 9-39) for treatment of post-bariatric hypoglycaemia. Diabetes Obes Metab 2020;22:1406–1416
25. Craig CM, Liu LF, Nguyen T, Price C, Bingham J, McLaughlin TL. Efficacy and pharmacokinetics of subcutaneous exendin (9-39) in patients with post-bariatric hypoglycaemia. Diabetes Obes Metab 2018;20:352–361
26. Ng CM, Tang F, Seeholzer SH, Zou Y, De León DD. Population pharmacokinetics of exendin-(9-39) and clinical dose selection in patients with congenital hyperinsulinism. Br J Clin Pharmacol 2018;84:520–532
27. Liu Q, Garg P, Hasdemir B, et al. Functional GLP-1R antibodies identified from a synthetic GPCR-focused library demonstrate potent blood glucose control. MAbs 2021;13:1893425
28. Gao Y, Peterson S, Masri B, et al. Cariprazine exerts antimanic properties and interferes with dopamine D2 receptor β-arrestin interactions. Pharmacol Res Perspect 2015;3:e00073
29. Griffith DA, Edmonds DJ, Fortin JP, et al. A small-molecule oral agonist of the human glucagon-like peptide-1 receptor. J Med Chem 2022;65:8208–8226
30. Chepurny OG, Bonaccorso RL, Leech CA, et al. Chimeric peptide EP45 as a dual agonist at GLP-1 and NPY2R receptors. Sci Rep 2018;8:3749
31. Chepurny OG, Matsoukas MT, Liapakis G, et al. Nonconventional glucagon and GLP-1 receptor agonist and antagonist interplay at the GLP-1 receptor revealed in high-throughput FRET assays for cAMP. J Biol Chem 2019;294:3514–3531
32. Carter PJ, Rajpal A. Designing antibodies as therapeutics. Cell 2022;185:2789–2805
33. Nauck MA, Quast DR, Wefers J, Meier JJ. GLP-1 receptor agonists in the treatment of type 2 diabetes - state-of-the-art. Mol Metab 2021;46:101102
34. Cary BP, Deganutti G, Zhao P, et al. Structural and functional diversity among agonist-bound states of the GLP-1 receptor. Nat Chem Biol 2022;18:256–263
35. Wootten D, Reynolds CA, Smith KJ, et al. The extracellular surface of the GLP-1 receptor is a molecular trigger for biased agonism. Cell 2016;165:1632–1643
36. Zhao P, Liang YL, Belousoff MJ, et al. Activation of the GLP-1 receptor by a non-peptidic agonist. Nature 2020;577:432–436
37. Cabrera O, Ficorilli J, Shaw J, et al. Intra-islet glucagon confers β-cell glucose competence for first-phase insulin secretion and favors GLP-1R stimulation by exogenous glucagon. J Biol Chem 2022;298:101484
38. Willard FS, Douros JD, Gabe MB, et al. Tirzepatide is an imbalanced and biased dual GIP and GLP-1 receptor agonist. JCI Insight 2020;5:e140532
39. Sun B, Willard FS, Feng D, et al. Structural determinants of dual incretin receptor agonism by tirzepatide. Proc Natl Acad Sci USA 2022;119:e2116506119
40. Wootten D, Christopoulos A, Marti-Solano M, Babu MM, Sexton PM. Mechanisms of signalling and biased agonism in G protein-coupled receptors. Nat Rev Mol Cell Biol 2018;19:638–653
41. Brekke OH, Thommesen JE. Tailoring natural effector functions. Antibody engineering beyond humanization. Methods Mol Biol 2003;207:383–391
42. Ryman JT, Meibohm B. Pharmacokinetics of monoclonal antibodies. CPT Pharmacometrics Syst Pharmacol 2017;6:576–588
43. Firan M, Bawdon R, Radu C, et al. The MHC class I-related receptor, FcRn, plays an essential role in the maternofetal transfer of gamma-globulin in humans. Int Immunol 2001;13:993–1002
44. Lu SC, Chen M, Atangan L, et al. GIPR antagonist antibodies conjugated to GLP-1 peptide are bispecific molecules that decrease weight in obese mice and monkeys. Cell Rep Med 2021;2:100263